Robert Tonndorf, Martin Kirsten, Rolf-Dieter Hund, Chokri Cherif

Designing UV/VIS/NIR-sensitive shape memory filament yarns

Erstveröffentlichung in / First published in:

Textile Research Journal. 2015, 85(12), S. 1305 – 1316 *[Zugriff am: 07.08.2019]*. SAGE journals. ISSN 1746-7748.

DOI: https://doi.org/10.1177/0040517514559578

Textile Research Journal

Review article

Textile Research Journal
2015, Vol. 85(12) 1305–1316

DOI: 10.1177/0040517514559578
trj.sagepub.com
SAGE

Designing UV/VIS/NIR-sensitive shape memory filament yarns

Robert Tonndorf, Martin Kirsten, Rolf-Dieter Hund and Chokri Cherif

Abstract

A novel laser light-sensitive yarn based on a thermoplastic polyester–urethane (TPU) has been prepared and analyzed. Since the thermosensitive shape memory polymer yarn (SMP yarn) has been functionalized using nanoscale heat sources exhibiting light-induced heat generation, the yarn is capable of an optically triggered shape memory effect (SME). For this purpose gold nanorods (GNR) have been employed. In addition to the incorporation of GNR into the yarn, a coating of GNR on the yarn is also proposed, applied by a semi-continuous layer-by-layer (LBL) technique. The SME of the functionalized yarns can be triggered either thermally or optically and has a strain recovery of almost 100%. The light-induced SME is triggered by a low-powered laser (808 nm, 2 W for a GNR-incorporated and 1 W for a GNR-coated TPU yarn). A reference yarn without GNR showed no significant effect. An adaptive structure featuring a SMP-yarn backed shape memory effect has been proposed and demonstrated.

Keywords

yarn, thermoplastic polyurethane, shape memory, nanoparticle, plasmon resonance, light-sensitive

A material which changes shape in a defined manner on stimulation is known as a shape-memory material. A well known example is the nickel–titanium alloy, Nitinol, discovered in 1963 by Buehler et al. at the US Naval Ordnance Laboratory.[1] Large-scale shape-change materials and composites include shape-memory alloys (SMA), liquid crystalline elastomers, hydrogels, conductive polymers, ferroelectric polymers, carbon nanotubes and shape-memory polymers (SMP).[2]All shape-memory materials have the ability to change their shape when triggered by an external stimulus. In contrast to SMAs, SMPs offer a high degree of deformation at low cost.[3,4]

For exploitation of the shape-memory effect (SME) the SMP is deformed into a secondary and temporary shape. The new shape is a metastable condition of the polymeric network and subsequent unloading does not restore it. Only when the material is activated by a specific stimulus, it does recover its original shape, and this is described as a one-way SME.[5] A range of stimuli may be used. Direct stimulation with heat,[6] light,[7,8] or water[9,10] may be effective, but heat is the most widely used stimulus. Alternatively, thermosensitive materials can be used, triggered by indirect stimuli such as electricity,[11] a magnetic field,[12,13] or light.[14,15]

Shape-memory yarns may be prepared by melt- or solvent-spinning.[16–20] Thermoplastic polyurethane (TPU) is widely used, since its mechanical properties offer a compromise between high modulus yarns such as nylon and high strain yarns like elastane.[16]

The linear chains of a TPU consist of two blocks, comprising hard and soft segments. Since the two segments are thermodynamically immiscible, a phase-separated network evolves.[21] The strength of the material is based on physical linkages between the hard segments of adjacent polymer chains.[22] The soft

Institute of Textile Machinery and High Performance Material Technology, Technical University of Dresden, Germany

Corresponding author:
Robert Tonndorf, Institute of Textile Machinery and High Performance Material Technology, Hohe Straße 6, Dresden, 01069, Germany.
E-mail: Robert.tonndorf@tu-dresden.de

segments are able to form a reversible semi-crystalline phase, and its reversibility can be employed as a trigger. Corresponding switching points are defined by the melting point (T_m) and the crystallization point (T_c) of the soft segment phase.

The permanent state of a TPU is characterized by a polymeric network of strongly coiled polymer chains and cross-linkages within both phases. At this stage the polymer exhibits a state of maximum entropy. As the TPU becomes loaded, strain-induced crystallization occurs within the soft segment phase, and the crystallization may be improved by cooling below the T_c. The new shape of the polymer is established by new physical cross-links; crystallites are formed within the soft segment phase, and the entropy of the polymeric network decreases. As the temperature within the metastable polymeric network rises above T_m the newly formed crystallites melt and entropy-driven shape recovery takes place (Figure 1).[5]

Indirect light-sensitive SMPs are discussed in the literature, and gold nanorods (GNRs) have been employed as additives in thermosensitive TPUs. An example is a nanocomposite prepared by the polymerization of monomers in the presence of GNRs and covalently attached polyethylene glycol chains (PEGylated GNRs).[14] The nanocomposite features a GNR concentration below 1 wt.% and is stimulated by laser light of wavelength 770 nm. Light stimulation increases the temperature of the material by 50 K, enabling shape recovery of the SMP. Another example is the combination of spherical gold nanoparticles and a SMP.[15] In this case the SME is triggered by laser light of wavelength 530 nm. In both approaches the particles convert light to heat by an effect described as localized surface plasmon resonance (LSPR).[23]A plasmon is a strong oscillation of the electron cloud within a metal nanoparticle induced by incident light. During resonance large amplitude oscillation occurs, together with strong light absorption. Due to collisions between ions, photons and electrons, heat is generated. If the nanoparticles are small, absorbance alone takes place and elastic scattering can be ignored.[24,25] The two absorption resonance wavelengths of the GNR are determined by the transverse and longitudinal LSPR, and the wavelength of the longitudinal LSPR is tunable by altering the aspect ratio of the GNRs.[26]

In the present study a TPU/GNR nanocomposite yarn has been fabricated, and can be remotely stimulated by a continuous wave laser operating at a specific frequency in the UV/VIS/NIR range (Figure 2). A wet-spun TPU yarn is formed, and is combined with GNRs of similar specific absorbance frequency. The method for functionalizing the yarn is intended to be a straightforward yarn finishing technique. In addition, a technical application is later described in which the SME is demonstrated in the form of a prototype.

Experimental details

Shape-memory filament yarn

A wet-spun filament yarn was prepared from TPU block copolymer pellets (Desmopan DP 2795A SMP; Bayer Material Science AG). The hard segments were comprised of 1,4-butanediol and the soft segments of PBA–3500, a pre-polymerized polyol of poly(1,4-butylene adipate) (PBA) of molecular mass 3500 g/mol.[27] Urethane linkages were provided by 4,4′-methylenediphenyl diisocyanate (MDI) (Figure 3). In order to determine whether the soft or the hard segment phase is dominant, elemental analysis (Hekatech EA 3000 Euro Vector CHNSO from the Department of

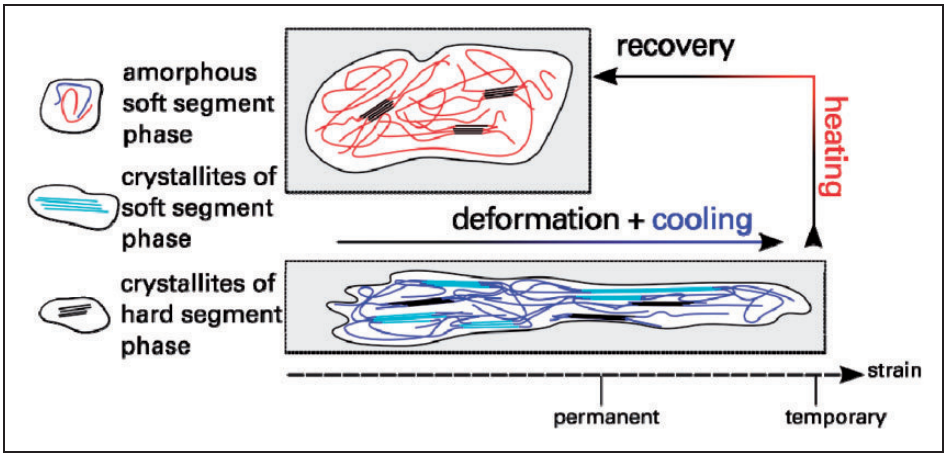

Figure 1. Macromolecular mechanism of the one-way shape memory effect.

Chemistry and Food Chemistry, TU Dresden) was conducted.

Yarn preparation was conducted using an established wet spinning technique on an in-house Pilot Wet Spintester from Fourné Polymertechnik GmbH. 300 g TPU pellets were dissolved in 1000 g dimethylformamide (DMF) and degassed at 60°C for 24 h. The polymer solution was carried from the reservoir through a filter to the spinneret (1500 holes, each 70 µm dia.) and spun into the coagulation bath, comprising water at 25°C. The yarn was tensioned and immediately passed through three washing baths (water at 30, 40 and 40°C) followed by passes through two ovens at 40°C. Finally, the processed yarn was wound into a coil.

The tensile strength of the yarn and its elongation at break were determined on a tensile tester Z2.5 (Zwick GmbH, Ulm, Germany), using 62.5 mm yarn samples at an initial load of 0.5 cN/tex and a displacement speed of 62.5 mm/min. The yarn samples were heat treated at 60°C prior to the experiment to recover the drawing effect during yarn preparation and processing.

The thermal properties of the TPU pellets and the yarn were determined by differential scanning calorimeter (DSC) measurement in a Q2000 (TA Instruments) in temperature modulated mode. Samples were analyzed over two cycles to avoid rearrangement mechanisms during first-time heating.[28] The sample was cooled to −35°C to equilibrate, then heated to 75°C and subsequently cooled to −35°C, then reheated to 280°C. The temperature modulation rate was ±0.50°C/40 s and the heating rate 20°C/min. Nitrogen was used for backflushing. T_m and T_c were determined from the change in latent heat output due to the irreversible heat flow.

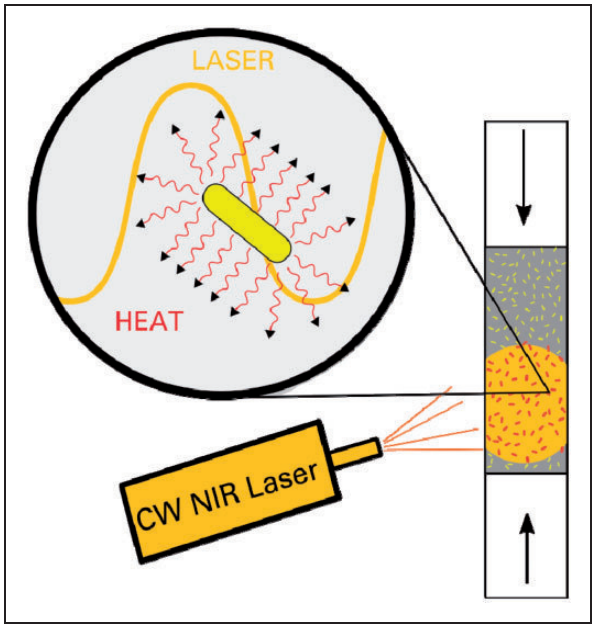

Figure 2. Scheme for the GNR/TPU nanocomposite.

Gold nanorods

GNR as additives were used for functionalization of the yarn. According to the method described by Nikoobakht,[29] GNR as synthesized have an absorbance maximum at 808 nm due to the longitudinal LSPR. A detailed description is given in Table 1. For all dilutions demineralized water was used. 5 ml of 0.2 M cetyltrimethylammonium bromide (CTAB) was mixed with 5 ml of 0.0005 M $HAuCl_4$, and to the mixture 0.6 ml freshly prepared ice-cold 0.01 M $NaBH_4$ was added and stirred for 2 h, giving CTAB-stabilized spherical gold nanoparticles as a seeding solution. 555 ml of 0.2 M CTAB, 555 ml of 0.001 M $HAuCl_4$, 7.77 ml of 0.0788 M AA and 25 ml of 0.004 M $AgNO_3$ were mixed to prepare the growth solution. 1.33 ml of

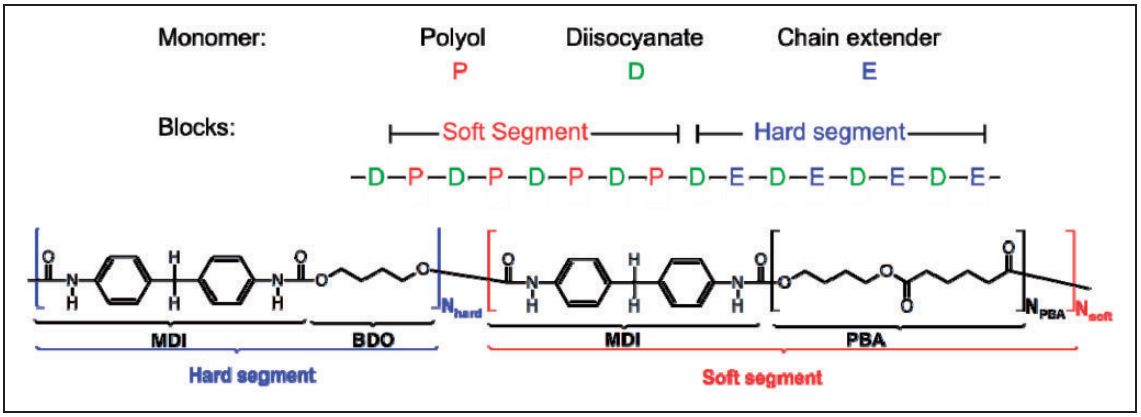

Figure 3. Block structure (top) and structural formula (lower) of a TPU.

Table 1. Chemicals employed for the synthesis of GNR

Chemical	Formula	CAS	Supplier
Cetyltrimethyl ammonium bromide (CTAB), ≥ 98%	$C_{19}H_{42}BrN$	57–09–0	Sigma–Aldrich
Gold(III) chloride trihydrate, ≥ 99.9% trace metals basis	$HAuCl_4$	16961–25–4	Sigma–Aldrich
Sodium borohydride, powdered	$NaBH_4$	16940–66–2	AppliChem
L(+)-Ascorbic acid (AA), food grade	$C_6H_8O_6$	50–81–7	AppliChem
Silver nitrate, ≥ 99.5%	$AgNO_3$	7761–88–8	Grüssing

the seeding solution was added to the growth solution and held for 2 h in a water bath (28°C). The volume of the GNR solution amounted to 1144 ml.

In order to remove traces of free CTAB, the GNR solution was washed twice with centrifugation, and the GNR were then surface-modified using a polyelectrolyte.[30] An aqueous solution of 35 wt.% sodium polyacrylate ([−CH_2−CH(COONa)−]; NaPA) of molecular mass 15000 g/mol was employed as a strong polyelectrolyte (Sigma–Aldrich). To increase the flexibility of the NaPA chains NaCl was employed. Solution S1 comprised 10 mg of NaPA per ml of 0.001 M NaCl, and solution S2 0.01 M NaCl, each prepared as water-based stock solutions. 0.2 ml of S1 and 0.1 ml of S2 were added drop-wise per ml of washed GNR solution. The NaPA/GNR solution was centrifuged to remove excess NaPA and the volume made up to 1150 ml with water.

Extinction spectra of the GNR solutions were plotted using a UV/VIS/NIR spectrophotometer, photoLab Spektral (WTW GmbH).

Yarn functionalization A

As a first attempt, NaPA/GNR was processed for incorporation into the yarn. The aqueous NaPA/GNR solution (1030 ml) was doubled in volume using DMF, the water removed as far as possible by rotary evaporation, and the volume made up to 1030 ml with DMF.

170 ml DMF and 300 g TPU pellets were added to the resulting solution to prepare a [NaPA/GNR]/TPU spinning solution, which was then used to prepare a second SMP yarn with GNR incorporated, employing the wet spinning technique described earlier under the heading, *Shape-memory filament yarn*.

Yarn functionalization B

The second functionalization method involved coating the pure yarn to form a GNR surface. For cationic surfactant-stabilized nanoparticles a simple layer-by-layer (LBL) coating was employed to form a thin layer of GNR on the wet-spun SMP yarn.

In a typical LBL method, alternating layers of oppositely charged polyelectrolytes (PE) or nanoparticles (NP) are deposited on a substrate.[31] The substrate is wetted in the order, [anionic PE or NP] → [H_2O] → [cationic PE or NP] → [H_2O] to give a single bilayer. H_2O removes loosely attached molecules or particles. By means of further wetting cycles, bilayers may be added. The LBL process has already been utilized for CTAB-stabilized dyes which are immobilized on a polymeric substrate,[32] and it has the potential to be regarded as an universal coating technique. Its drawback is the time it requires, which is governed by the rate of molecular adsorption by the substrate. For this reason spray coating rather than dip-coating has been proposed.[33] In here, SMP yarn functionalization was achieved by a similar LBL technique. About 30 m of pure TPU yarn (see section: *Shape-memory filament yarn*) was used for functionalization.

Anionic NaPA-stabilized GNR were combined with a cationic polyvinylamine polyelectrolyte (Lupamin 9095, BASF; PVAm) of molecular mass 340.000 g/mol. For 200 ml of cationic PE solution, the PVAm was diluted with water to 10 mg/ml and rendered alkaline (pH 9) using NaOH, to increase the thickness of the subsequent PVAm layer.[36] 113 ml of the NaPA/GNR solution (see section: *Gold nanorods*) was used in forming the anionic layer. Washing was employed with 2 × 200 ml water.

A cationic PVAm primary layer was initially formed on the hydrolyzed TPU yarn. Hydrolysis was employed using 1 M sodium hydroxide solution at 40°C for 5 h, followed by washing. This resulted in the presence of carboxylate anions on the surface of the yarn.[34,35]

Deposition of the yarn was achieved by transporting the yarn at 5 m/min through glass beakers containing the polyelectrolytes, followed by an oven at 80°C, and finally coiling. Similar to the spinning process, the yarn was tensioned during the process. The first deposition cycle served for coating of the primary layer in the sequence: PVAm → H_2O→ drying → coiling. 10 further bilayers of NaPA/GNR and PVAm were

formed in the sequence: [NaPA/GNR→ H_2O→ PVAm → H_2O→ drying → coiling] × 10.

Carboxylate anions of the hydrolyzed TPU-yarn were analyzed by a Fourier-transform infrared (FT–IR) spectrometer (Nicolet 6700, Thermo Fisher Scientific, USA). In order to confirm the formation of a thin NaPA/GNR and PVAm multilayer, SEM images were taken at the Leibniz Institute of Polymer Research, Dresden.

For both functionalized yarns A and B the gold mass fraction was determined by atomic absorption spectrometry (AAS; ZEEnit 700, Analytik Jena). A segment of known mass of each yarn was dissolved in 10 ml aqua regia (concentrated sulfuric acid: hydrochloric acid in a volume ratio 1:3) for 24 h. Spectroscopic measurements were performed on a 1 ml drop of the solution, further diluted with water by a factor of 100. For each solution three measurements were conducted.

Shape–memory effect

The SME is indirectly triggered by light, but directly triggered by heat. For this reason heat generation within the yarn induced by laser light was examined using a 808 nm laser diode RLTMDL–808–2 W (Roithner Lasertechnik GmbH) over a range of power input. At the aperture the laser beam was 5 × 8 mm, and yarn samples were illuminated vertically at a distance of 20 cm (beam divergence <3.0 mrad). The heat generated was measured by temperature change analysis using an infrared camera, Pyroview 380 L compact (DIAS Infrared Systems). Five yarn samples of each type of functionalized yarn were weighted and located in front of the laser. Illumination took place over 60 s, and the maximum temperature was assessed by the camera software, room temperature being recorded as 25°C. The influence of radiation power was determined by varying the laser power applied (0.5, 1.0 or 2.0 W).

SME properties were observed in thermo-mechanical cycles, each cycle comprising deformation, fixation and recovery. The cycles were analyzed using the tensile testing machine Z2.5 (Zwick) in terms of strain fixation (Equation 1) and strain recovery (Equation 2). Both were determined in the fourth of four successive thermo-mechanical cycles. For comparison, direct heat, indirect light and no stimulation were included. The yarn samples had a length of 40 mm and were heat treated at 60°C prior to the experiment to recover the drawing effect during yarn preparation.

$$R_f = \frac{\varepsilon_f - \varepsilon_0}{\varepsilon_m - \varepsilon_0} \quad (1)$$

$$R_r = \frac{\varepsilon_m - \varepsilon_r}{\varepsilon_m - \varepsilon_0} \quad (2)$$

where ε_0 was the initial strain, ε_m the maximum strain, ε_f the fixed strain, and ε_r the recovered strain.

In one thermo-mechanical cycle (Figure 4) the samples were extended to 100% at a speed of 30 mm/min

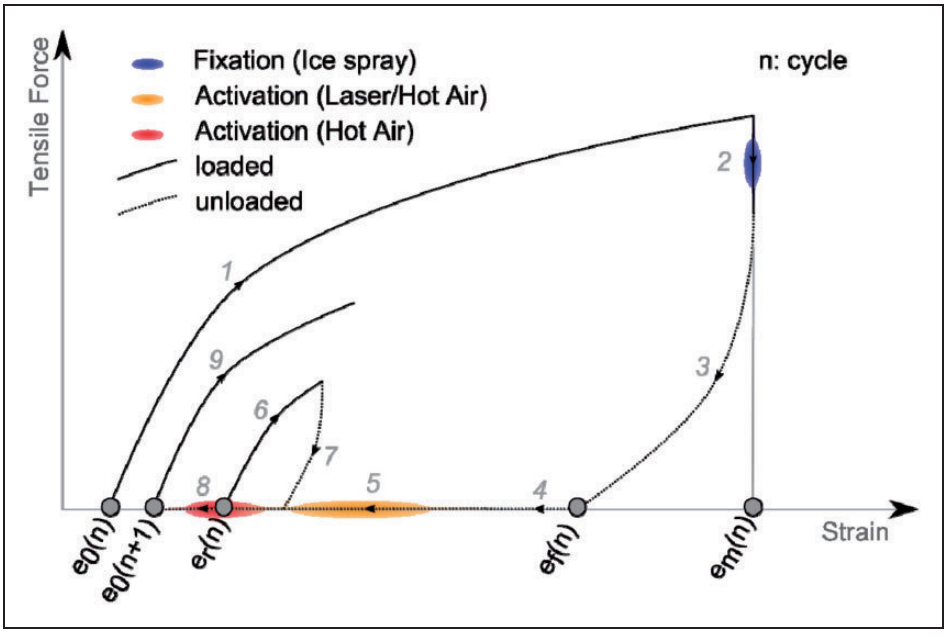

Figure 4. Sketch of the thermo-mechanical cycle for characterization of the shape-memory effect.

without initial force (step 1). The stretched samples were fixed by the application of a cooling spray (Kälte 75, CRC KontaktChemie) (step 2), and then held unloaded in clamps for 5 min, as the clamps being positioned to the initial gap (steps 3–4). For heat stimulation a hot air gun (HL 2010 E, Steinel) operating at 60°C was used, with a yarn sample paling cap, and the laser was used for light stimulation (step 5). Stimulation was applied for 60 s with the samples enclosed within the cap, and the laser beam was guided twice over the yarn sample. Following the stimulation step, the recovered strain was measured by straining the samples to 50% (step 6). Finally, the clamps were positioned to the initial gap (step 7) and the samples were treated with hot air at 60°C to ensure that the yarn had fully recovered for the following cycle (step 8). The following cycle began with step 9. All thermo-mechanical cycles were conducted three times for each yarn type, and measurements were performed to an accuracy of ±0.5 mm.

Results and discussion

Shape-memory filament yarn

The weight fractions of carbon, hydrogen and nitrogen were determined by elemental analysis, and oxygen by calculation (Table 2). The polymer was treated statistically as a block copolymer, as seen in Figure 3. Based on this chemical structure, hard and soft segment fractions should theoretically vary between 0% and 100%. For each theoretical chemical composition the elemental fraction was calculated and compared with the results of CHNO analysis. Comparison with the smallest error gave a composition comprising a weight fraction of 84% soft and 16% hard segments. From this estimate it was clear that the soft segment phase was dominant within the polymeric network.

A wet spun TPU yarn was successfully prepared, and the average linear mass density of 962 tex, average elongation at break of 430 ± 26% and average tensile strength of 4.2 ± 0.4 cN/tex were determined. The tensile test revealed high deformation, but the low tensile strength was probably the result of the high proportion of soft and low proportion of hard segments.

The first heating cycle of DSC measurements differed from the second cycle, due to rearrangement of the phase structure (Figure 5). The second cycle was therefore used for determination of the characteristic switching temperature, T_m. Characteristic peaks were seen in the range −20°C to 60°C, attributed to the crystallization and melting of the soft segment phase. In

Table 2. Results of elemental analysis

Element	H	C	N	O
M/wt.%	7.6	61.5	2.1	28.8*

*calculated

Table 3. Thermal properties of TPU pellets and yarn

Type	T_c (°C)	T_m (°C)
Pellets	2.4	37.4
Yarn	2.2	38.9

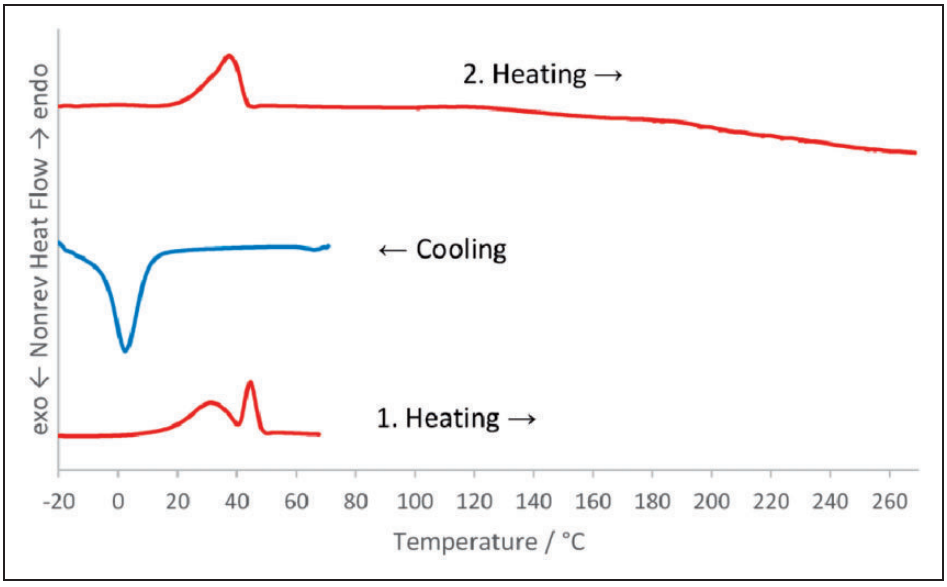

Figure 5. DSC measurements of TPU pellets.

Table 3 the characteristic values of DSC measurements are listed. T_m as an indicator of the activation temperature was 40°C. T_c, which is required for the fixation of the strained material, was close to 0°C, thus implying that a thermal hysteresis of almost 40°C was present. In addition, no high temperature melting peak was apparent, which would have been due to the melting of crystallites in the hard segment phase. The absence of this melting peak was probably not particularly significant, however, as the polymer had a low hard segment phase fraction. It can also be concluded that the wet spinning process of the TPU did not affect the switching temperature, as the thermal properties of the spun polymer remained unaltered (Table 3).

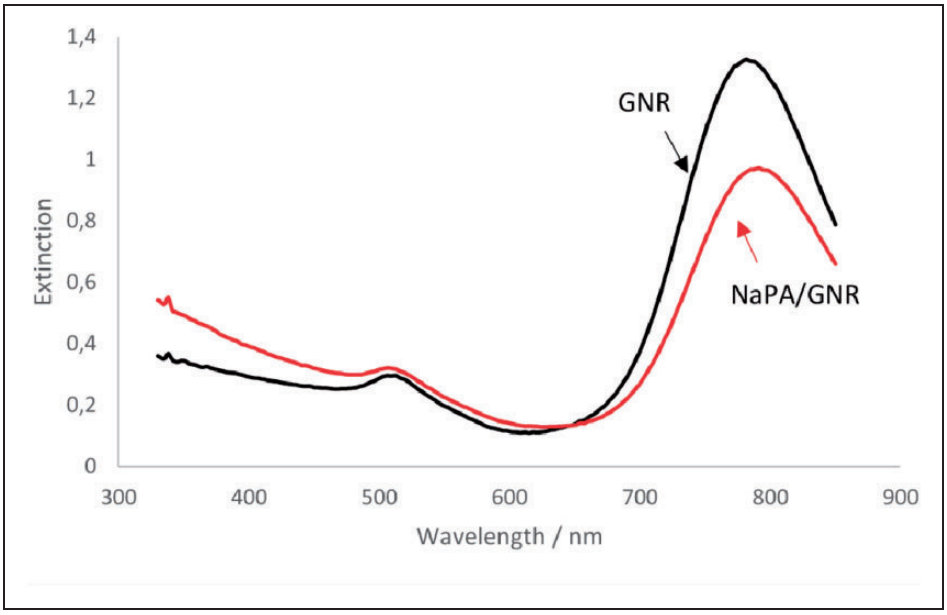

Figure 6. Extinction spectrum of the GNR and NaPA/GNR dispersions.

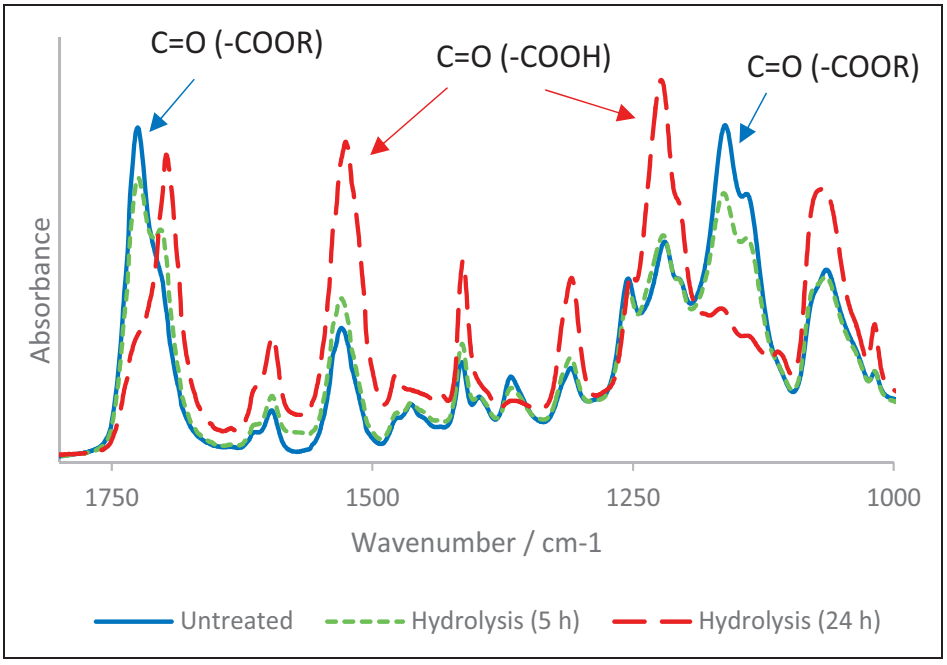

Figure 7. FTIR spectra of the alkali-treated yarn.

Gold nanorods

The extinction spectrum of the GNR dispersion showed two peaks (Figure 6), which may be attributed to the transverse (510 nm) and longitudinal LSPR (780 nm). Further processing of the GNR solution decreased the intensity of the peaks by about 25%, but a strong absorbance remained at 808 nm.

Yarn functionalization

GNR were coated with the polyelectrolyte NaPA to allow phase transfer into the DMF; the color of the solution remained unchanged, although a few precipitated agglomerates could be seen.

Although a water/DMF azeotrope was formed after the phase transfer of GNR into DMF, the added TPU passed into solution, further enabling wet spinning. The incorporation of GNR by straightforward mixing successfully achieved a functionalized yarn.

For the second functionalization approach hydrolysis was carried out on the surface of the yarns. As shown in Figure 7, alkali treatment led to the presence of carboxyl groups. The formation of carboxyl groups by alkaline hydrolysis of the ester groups was confirmed by extended treatments of up to 24 h, and as a result the stretching vibration of the carbonyl group (C = O) in the ester group (−COOR) decreased in favor of the stretching vibration of C = O in the carboxyl groups (−COOH).

Subsequent LBL coating was performed in a semi-continuous manner. The volume of the GNR bath decreased by about 90 ml, the reddish coloring of the subsequent baths indicating that GNR had been extracted and carried through to the following baths. After deposition of 10 bilayers the resulting yarn also showed a reddish color, suggesting immobilization of GNR on the yarn surface.

On the SEM images it was observed that the untreated TPU yarn had a smooth surface, whereas following LBL coating it had a rough surface (Figure 8). The wrinkled surface of the coating was probably a consequence of the processing steps. The yarn was in a strained condition after spinning and the LBL coating was applied to the pre-strained yarn. Subsequent contraction of the unloaded yarn samples for SEM resulted in wrinkling of the surface coating, as it was not able to contract. Although no heating was involved, shape recovery took place (see section: Shape-memory effect). However, the BSE image shows fine dispersed dots with bright contrast, attributed to GNR within a nanoscale layer less than 200 nm in thickness. In addition, it was observed that the filament cross-section was not circular.

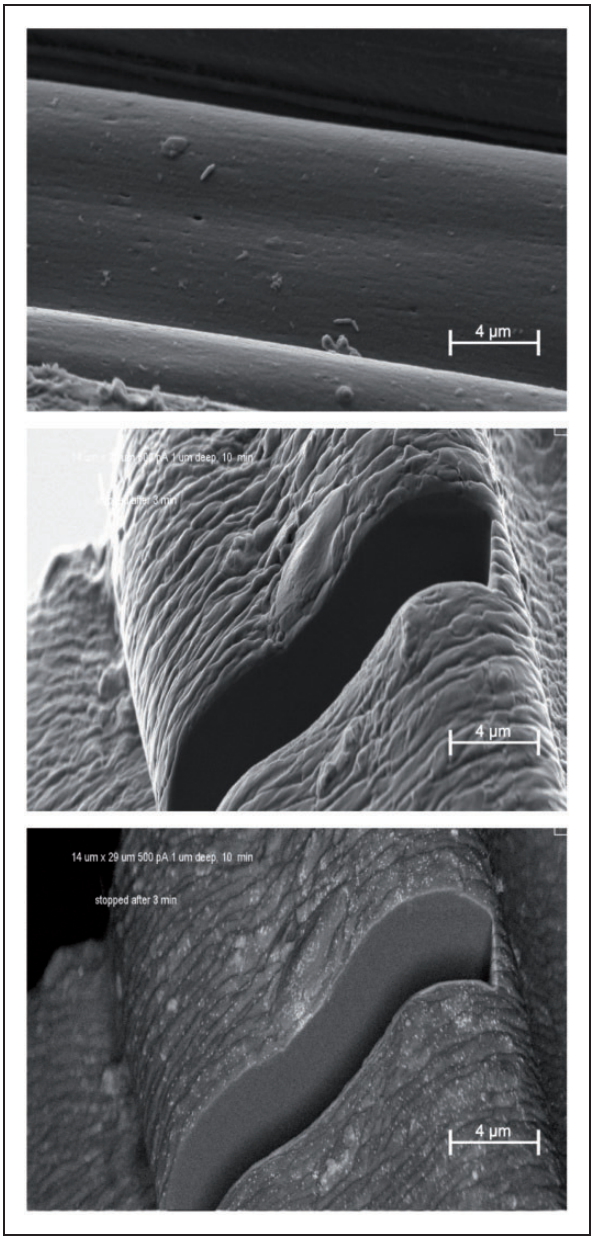

Figure 8. SEM images of the pure TPU yarn (top) and immobilized GNR within a nanoscaled layer on the TPU multifilament yarn, by secondary electron analysis (middle) and backscattered electron analysis (bottom).

AAS measurements indicated the amount of GNR within the functionalized yarns. It should be noted that for each functionalized yarn a similar amount of gold was initially used (0.3 mg of gold per g of TPU, corresponding to 300 wt. ppm). The gold to polymer fraction after incorporation was 13.5 ± 0.9 wt. ppm, and after coating it became 44.0 ± 1.1 wt. ppm, assuming the gold atoms were attributable to the GNR. It is clear that the LBL coating procedure was more efficient, since the gold fraction was more than three times

greater relative to the quantity incorporated. The increased gold loss during the incorporation procedure could be attributed to the centrifugation steps, and in particular to the phase transfer, during which agglomerates were formed. As a result, GNR agglomerates were lost by precipitation, or were possibly non-homogeneously dispersed within the polymer matrix and consequently not detected by AAS. The losses during the coating procedure could also be attributed to the centrifugation steps and the drawing during yarn wetting.

Shape-memory effect

Temperature measurements during laser light illumination at 2 W indicated heat generation in the presence of GNR (Table 4). The minor temperature change from 25 to 33°C of the illuminated pure TPU yarn suggested that at a wavelength of 808 nm the polymer was semi-transparent. On the other hand the temperature of the GNR-filled yarn increased to 45°C, and in the case of the GNR-coated yarn the temperature increased to above 100°C. In view of its activation temperature of 40°C the SME would not be triggered for the pure yarn, and a power of 2 W was required for the incorporated yarn and 1 W for the coated GNR/SMP yarn.

Table 4. Temperature change of the yarn on laser light illumination at room temperature (25°C)

Laser P (W)	Reference, no GNR T_{Ref} (°C)	Incorporated GNR T_{Inc} (°C)	Coated GNR T_{Coat} (°C)
0.5	26.2	28.7 ± 0.9	38.5 ± 3.6
1.0	28.8	35.2 ± 1.4	72.6 ± 7.6
2.0	33.3	44.8 ± 1.7	106.9 ± 4.5

Thermal response due to laser light illumination was expected to occur only locally, since polymers are weak thermal conductors. In Figure 9 it is seen that the heat was not dispersed, and in addition that a temperature increase or decrease was the immediate result of the laser beam, since the heat capacity of the yarn was low.

The effectiveness of the SME was revealed in the strain fixation, R_f, describing the ability of obtaining and retaining a deformed state, and in the strain recovery, R_r, which characterizes the ability to return from the strained state back to the initial permanent strain. Characteristic values are typically obtained from the thermo-mechanical cycle, in which the first cycle differs from those following. Consequently more than one cycle was run, in which the values converged. In Figure 10 the upper curve shows how the first cycle differed from the other three similar curves, and in Table 5 the values of R_f and R_r during the fourth cycle are summarized.

It is clear that strain fixation occurred when no cooling spray was applied, due to strain-induced crystallization within the soft segment phase (#1 in Table 5). Further cooling increased the number of crystallites in this phase, resulting in increased fixation (#2 in Table 5). The strain recovery was almost complete when the yarn was stimulated by hot air, whether it was a pure TPU or a functionalized yarn (#3, #5, #8 in Table 5). When no stimulation was applied recovery was significantly lower (#2 in Table 5). It is also

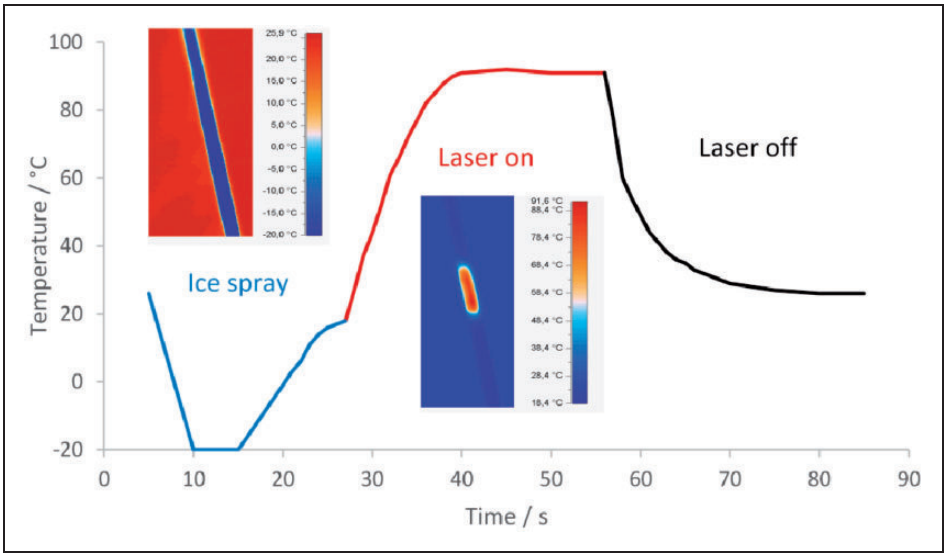

Figure 9. Temperature–time diagram for cooling and laser light illumination. The insets show thermal images from the infrared camera.

apparent from the data that the fixation values were scattered, which is a feature of manual application of the cooling spray.

Laser light-induced SME experiments helped to clarify the results of laser-induced heat generation. The degree of strain recovery depended both on the applied laser power and the GNR fraction. Since recovery was triggered when laser light stimulation induced a temperature increase within the material, a strong correlation between both data sets (Tables 4 and 5) is understandable. Recovery values of almost 100% were achieved at a laser power of 2 W for the yarn with GNR incorporated, and by a power of 1 W for the GNR-coated yarn (#7, #10 in Table 5 and Figure 11). Full recovery was not observed at lower laser power (#6, #9 in Table 5).

It is concluded that the SMP yarn can be activated either by heat or by light, if a laser of suitable power is applied to the GNR-functionalized SMP yarn.

Table 5. Strain fixation R_f and recovery R_r for the fourth thermo–mechanical cycle

#	Yarn sample	Fixation	Stimulation	R_f (4) (%)	R_r (4) (%)
1	TPU	–	Heat	67 ± 10	100 ± 5
2	TPU	Spray	–	92 ± 16	22 ± 8
3	TPU	Spray	Heat	89 ± 6	100 ± 5
4	TPU	Spray	Laser (1 W)	76 ± 4	34 ± 10
5	TPU/GNR (inc.)	Spray	Heat	79 ± 8	100 ± 5
6	TPU/GNR (inc.)	Spray	Laser (1 W)	79 ± 3	65 ± 4
7	TPU/GNR (inc.)	Spray	Laser (2 W)	81 ± 9	97 ± 7
8	TPU/GNR (coat.)	Spray	Heat	89 ± 8	100 ± 5
9	TPU/GNR (coat.)	Spray	Laser (0.5 W)	91 ± 3	61 ± 4
10	TPU/GNR (coat.)	Spray	Laser (1 W)	91 ± 4	99 ± 7

Prototype

For SMP yarns a range of textile-based application may be proposed,[37,38] including wrinkle-free fabrics or those embodying temperature or moisture control. A yarn-based application is also suggested as a smart suture for minimally invasive surgery, in which the knot fastening includes a SME.[39]

The motivation for a SMP yarn-based structure may be traced back to lightweight deployable structures. These structures can be implemented by tensegrities, which are three-dimensional structures composed of poles and tensile elements.[40]

In this case the tensile elements are made up of SMP yarns. If these are highly deformed and fixed, the connected poles and yarns do not allow flow of the forces, and the tensegrity becomes unstable and foldable. As SMP yarn stimulation is applied, the tensile elements contract and the structure adopts a defined three-dimensional shape. For a light-sensitive yarn, remotely triggered activation by a frequency-specific laser is also possible, and a well-defined deployment over long source-to-object distances becomes practicable. For demonstration purpose the folded tensegrity may be placed in an oven at 60°C, deployment occurs within a matter of seconds (Figure 12, and video).

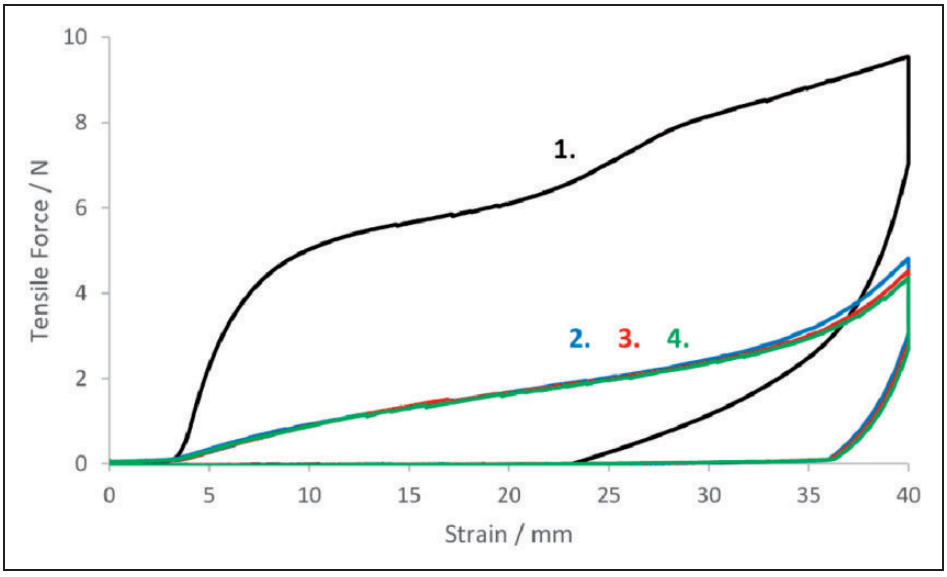

Figure 10. Stress–strain curves of thermo-mechanical cycles of the TPU yarn. For clarity steps 6–8 are not shown (see Figure 4).

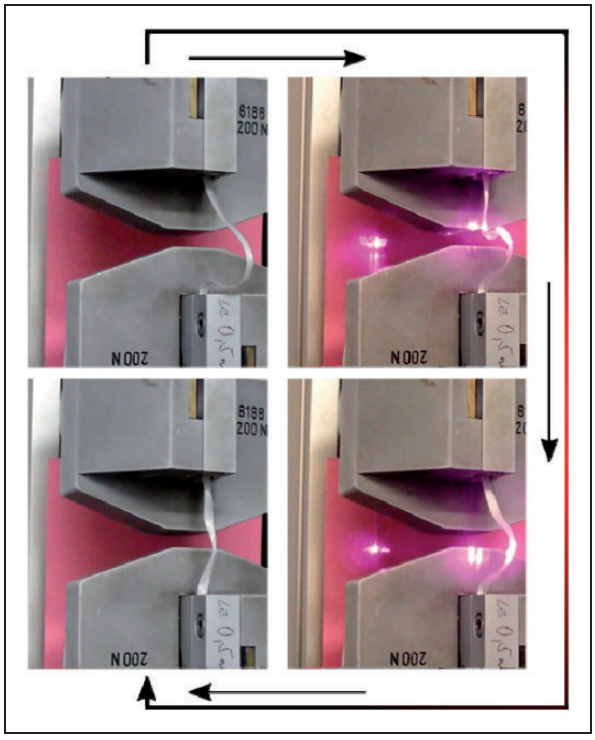

Figure 11. Laser light-induced strain recovery of a strained GNR-functionalized TPU yarn.

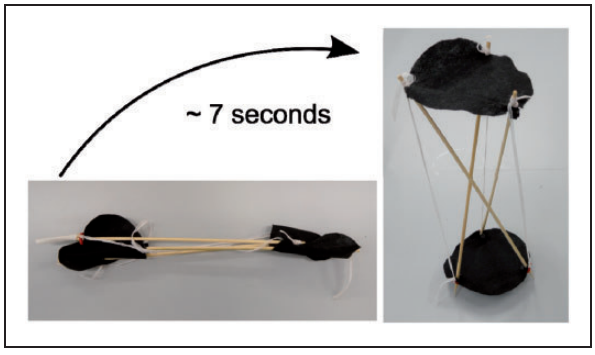

Figure 12. Deployment of a tensegrity upon heat stimulation.

Conclusions

A SMP yarn has been successfully prepared by a wet spinning technique. The yarn was functionalized by the incorporation of GNR within the yarn, or by coating GNR on its surface. Both these functionalization methods are straightforward and can be applied during conventional spinning and finishing. The SME of the functionalized yarns was triggered at 40°C, and direct heat or indirect light stimulation were equally effective. Light-induced SME depends on the GNR fraction of the nanocomposite yarn and on the laser power applied. Since significantly more GNR losses occur during GNR incorporation processing, a LBL-coating method is preferred. SMP yarns may be utilized in adaptive structures to perform heat-triggered deployment, in which activation is remotely triggered by the incorporation of light-sensitive yarns.

Acknowledgements

The authors are grateful to Michael Posselt for the wet spinning, Dr Heike Hund for AAS-measurements, Tina Heidrich for tensile tests, Bayer Material Science AG for the supply of the shape-memory polymer and Dr Petr Formanek of the Leibniz Institute of Polymer Research, Dresden, for the SEM images.

The research received no specific grant from any funding agency within the public, commercial, or not-for-profit sectors.

References

1. Kumar P and Lagoudas D. Introduction to shape memory alloys. In: D. C. Lagoudas (eds) Shape Memory Alloys: Springer US; 2008: 1–51.
2. Madden J, Vandesteeg N, Anquetil P, Madden P, Takshi A, Pytel R, et al. Artificial muscle technology: physical principles and naval prospects. *IEEE J Oceanic Eng*. 2004; 29(3): 706–728.
3. Liu C, Qin H and Mather PT. Review of progress in shape-memory polymers. *J Mater Chem* 2007; 17(16): 1543–1558.
4. Rousseau IA. Challenges of shape memory polymers: A review of the progress toward overcoming SMP's limitations. *Polym Eng Sci* 2008; 48(11): 2075–2089.
5. Lendlein A. Shape-memory polymers. Advances in Polymer Science, ed. Heidelberg: Springer-Verlag Berlin; 2010.
6. Auad ML, Mosiewicki MA, Richardson T, Aranguren MI and Marcovich NE. Nanocomposites made from cellulose nanocrystals and tailored segmented polyurethanes. *J Appl Polym Sci* 2010; 115(2): 1215–1225.
7. Lendlein A, Jiang H, Jünger O and Langer R. Light-induced shape-memory polymers. *Nature* 2005; 434: 879–882.
8. Jiang HY, Kelch S and Lendlein A. Polymers move in response to light. *Adv Mater* 2006; 18(11): 1471–1475.
9. Chae JY, Hwa SH and Whan CJ. Water-responsive shape memory polyurethane block copolymer modified with polyhedral oligomeric silsesquioxane. *J Macromol Sci Phys* 2006; 45(4): 453–461.
10. Huang WM, Yang B, Zhao Y, et al. Thermo-moisture responsive polyurethane shape-memory polymer and composites: a review. *J Mater Chem* 2010; 20(17): 3367–3381.
11. Gunes IS, Jimenez GA and Jana SC. Carbonaceous fillers for shape memory actuation of polyurethane composites by resistive heating. *Carbon* 2009; 47(4): 981–997.
12. Mohr R, Kratz K, Weigel T, et al. Initiation of shape-memory effect by inductive heating of magnetic

nanoparticles in thermoplastic polymers. *P Natl Acad Sci USA* 2006; 103(10): 3540–3545.
13. Razzaq MY, Anhalt M, Frormann L, et al. Thermal, electrical and magnetic studies of magnetite filled polyurethane shape memory polymers. *Mat Sci Eng A–Struct* 2007; 444(1): 227–235.
14. Hribar KC, Metter RB, Ifkovits JL, et al. Light-induced temperature transitions in biodegradable polymer and nanorod composites. *Small* 2009; 5(16): 1830–1834.
15. Zhang H, Xia H and Zhao Y. Optically triggered and spatially controllable shape-memory polymer–gold nanoparticle composite materials. *J Mater Chem* 2012; 22(3): 845–849.
16. Zhu Y, Hu J, Yeung LY, et al. Development of shape memory polyurethane fiber with complete shape recoverability. *Smart Mater Struct* 2006; 15(5): 1385.
17. Meng Q, Hu J, Zhu Y, et al. Polycaprolactone-based shape memory segmented polyurethane fiber. *J Appl Polym Sci* 2007; 106(4): 2515–2523.
18. Kaursoin J and Agrawal AK. Melt spun thermoresponsive shape memory fibers based on polyurethanes: Effect of drawing and heat-setting on fiber morphology and properties. *J Appl Polym Sci* 2007; 103(4): 2172–2182.
19. Ji F, Zhu Y, Hu J, et al. Smart polymer fibers with shape memory effect. *Smart Mater Struct* 2006; 15(6): 1547.
20. Meng Q, Hu J, Zhu Y, et al. Morphology, phase separation, thermal and mechanical property differences of shape memory fibres prepared by different spinning methods. *Smart Mater Struct* 2007; 16(4): 1192.
21. Bagdi K, Molnár K, Kállay M, et al. Quantitative estimation of the strength of specific interactions in polyurethane elastomers, and their effect on structure and properties. *Eur Polym J* 2012; 48(11): 1854–1865.
22. Lee BS, Chun BC, Chung YC, et al. Structure and thermomechanical properties of polyurethane block copolymers with shape memory effect. *Macromolecules* 2001; 34(18): 6431–6437.
23. Chou CH, Chen CD and Wang CC. Highly efficient, wavelength-tunable, gold nanoparticle based optothermalnanoconvertors. *J Phys Chem B* 2005; 109(22): 11135–11138.
24. Sönnichsen C. Plasmons in metal nanostructures. PhD Thesis, LMU München, Germany, 2001.
25. Stockman MI. Nanoplasmonics: the physics behind the applications. *Phys Today* 2011; 46(2): 39–44.
26. Link S and El-Sayed MA. Spectral properties and relaxation dynamics of surface plasmon electronic oscillations in gold and silver nanodots and nanorods. *J Phys Chem B* 1999; 103(40): 8410–8426.
27. Pretsch T, Jakob I and Müller W. Hydrolytic degradation and functional stability of a segmented shape memory poly(ester urethane). *Polym Degrad Stabil* 2009; 94(1): 61–73.
28. Auad ML, Richardson T, Hicks M, et al. Shape memory segmented polyurethanes: dependence of behavior on nanocellulose addition and testing conditions. *Polym Int* 2012; 61(2): 321–327.
29. Nikoobakht B and El-Sayed MA. Preparation and growth mechanism of gold nanorods (NRs) using seed-mediated growth method. *Chem Mater* 2003; 15(10): 1957–1962.
30. Alkilany AM, Thompson LB and Murphy CJ. Polyelectrolyte Coating Provides a Facile Route to Suspend Gold Nanorods in Polar Organic Solvents and Hydrophobic Polymers. *ACS Appl Mater* 2010; 2(12): 3417–3421.
31. Srivastava S and Kotov NA. Composite layer-by-layer (LBL) assembly with inorganic nanoparticles and nanowires. *Accounts Chem Res* 2008; 41(12): 1831–1841.
32. Malikova N, Pastoriza-Santos I, Schierhorn M, et al. Layer-by-layer assembled mixed spherical and planar gold nanoparticles: control of interparticle interactions. *Langmuir* 2002; 18(9): 3694–3697.
33. Izquierdo A, Ono SS, Voegel JC, et al. Dipping versus spraying: exploring the deposition conditions for speeding up layer-by-layer assembly. *Langmuir* 2005; 21(16): 7558–7567.
34. Liu Y, He T and Gao C. Surface modification of poly (ethylene terephthalate) via hydrolysis and layer-by-layer assembly of chitosan and chondroitin sulfate to construct cytocompatible layer for human endothelial cells. *Colloid Surface B* 2005; 46(2): 117–126.
35. Liu Y, He T, Song H and Gao C. Layer-by-layer assembly of biomacromolecules on poly (ethylene terephthalate) films and fiber fabrics to promote endothelial cell growth. *J Biomed Mater Res A* 2007; 81(3): 692–704.
36. Elzbieciak M, Kolasinska M and Warszynski P. Characteristics of polyelectrolyte multilayers: The effect of polyion charge on thickness and wetting properties. *Colloid Surface A* 2008; 321(1): 258–261.
37. Hu J, Meng H, Li G and Ibekwe SI. A review of stimuli-responsive polymers for smart textile applications. *Smart Mater Struct* 2012; 21(5): 053001.
38. Hu J and Chena S. A review of actively moving polymers in textile applications. *J Mater Chem* 2010; 20(17): 3346–3355.
39. Lendlein A and Langer R. Biodegradable, elastic shape-memory polymers for potential biomedical applications. *Science* 2002; 296(5573): 1673–1676.
40. Tibert G. Deployable tensegrity structures for space applications. PhD Thesis. Royal Institute of Technology, Sweden, 2002.